Theory of longitudinal Schottky spectra of ordered ion beams in a storage ring

V. V. Avilov* and I. Hofmann
Gesellschaft für Schwerionenforschung Darmstadt, D-6100 Darmstadt, Germany
(Received 11 March 1992; revised manuscript received 23 September 1992)

The longitudinal Schottky spectrum of an ultracold ion beam in a storage ring is calculated in the frame of harmonic oscillations of a one-dimensional (1D) Coulomb lattice. It is assumed that the extremely high cooling rate required to bring the beam into a one-dimensional ordered chain can be provided by electron or laser cooling. The anharmonic transversal oscillations with temperature much higher than the longitudinal one are taken into account within the self-consistent phonon approximation. The Schottky spectrum measured by the pickup system consists of bands located near the harmonics of the revolution frequency of the beam. The total intensity of each band characterizes the temperature distribution of the phonons in an ionic chain. The amplitude and the width of the peaks in the spectrum are a function of the strength of relaxation processes (cooling and heating) and the Coulomb correlations, respectively. It is suggested that a careful analysis of these spectra could be a signature of the presence of 1D ordering in the beam.

PACS number(s): 41.75.Ak, 29.20.Dh

I. INTRODUCTION

Electron-cooling experiments by Dementev *et al.* at Novosibirsk [1] and more recently in the TSR storage ring at Heidelberg by Jaeschke *et al.* [2] and in the ESR storage ring at GSI by Franzke [3] have shown that extremely small momentum spreads (below 10^{-6}) are possible for small intensities (typically 10^5–10^6 ions). The temperatures of such beams are of the order of 1 K in beam direction, but are several orders of magnitude higher transversely. Even lower temperatures (tens of mK) can be achieved with laser cooling, which works in the longitudinal direction [4,5]. Coulomb scattering ("intrabeam scattering") of the ions from the transverse direction may result in longitudinal heating, which is assumed in all these experiments to limit the minimum achievable momentum spread. In the longitudinal phase plane one thus expects a dynamical equilibrium, which is a result of the combined effect of cooling and intrabeam scattering heating. The pioneering experiments with cooled proton beams at Novosibirsk by Dementev *et al.* have suggested, on the other hand, that after careful optimization of the cooling device and low enough intensities the intrabeam scattering is possibly suppressed due to ordering effects of the ions along their equilibrium orbit [1]. Computer simulation using molecular dynamics also indicates that for certain parameters the intrabeam scattering heating is strongly reduced such that the longitudinal "temperature" adopts values low enough to allow longitudinal ordering [6]. The dimensionless parameter that determines the conditions for ordering is the ratio of the Coulomb energy of the lattice to the temperature

$$\Gamma=\frac{(eZ)^2}{dT}\ , \tag{1.1}$$

where Z is the ion charge and d the interionic distance. This coupling parameter Γ, defined with the longitudinal temperature, must exceed unity in such a situation. Such values are consistent with the measured longitudinal temperatures, but not the transverse ones. They also confirm theoretical calculations on the minimum achievable momentum spread and Γ values in electron cooling [7].

Considerations of such highly cooled heavy-ion beams have led to the prediction that a transition to a crystalline structure might occur if the temperature of the beam is small enough [8]. More detailed calculations have shown that such a transition is difficult to achieve in a storage ring where the beam has a large forward energy compared with the temperatures in the beam frame and bending is involved which exerts a shear on the particle motion [9]. The discrete lattice of a strong focusing storage ring, in particular, was found to introduce enough heating that crystalline three-dimensional (3D) states would seem to be unlikely to occur [10].

If the number of particles in the storage ring is below a certain threshold an ordered structure could be a simple linear chain of ions [11], which is more likely to be achievable in a strongly focusing ring [10]. For observation it is necessary to determine the temperature, energy distribution, and structure of the ion beam. The most useful method of beam diagnostics is the analysis of the Schottky spectrum measured by a pick-up system. The general theory of Schottky signals is developed in detail in Refs. [12–15] for the case of the plasma approximation. The aim of the present paper is to calculate the Schottky spectrum of beams with internal ordering. As we can see in Sec. II the Schottky spectrum may be expressed in terms of the dynamical structure factor of the system.

The dynamical structure factor is one of the most widely used characteristics of the crystal in condensed matter physics. There exists extensive literature describing methods of calculation of the dynamical structure factor and the application of these methods to the experimental study of x-ray or neutron scattering in solids and liquids (see, for example, Refs. [16,17]). Also, during the

past two decades intensive theoretical and experimental studies of some types of quasi-one-dimensional crystals have been carried out [18,19]. It has been shown that the dynamical structure factor of an infinite atomic chain is quite different from the case of 3D crystals. The aim of the present paper is to analyze some peculiarities of the phonon spectrum of the ordered ionic chain and obtain the Schottky spectrum for it.

For ion beams in a storage ring there are additional peculiarities, and we must take into account in our calculations the following.

(a) The interaction of the ions is described by the Coulomb force, which is a long-range force.

(b) The ion beam in a storage ring is not an infinite chain, but a circle of typically 10^5 or more ions.

(c) This system can have distinct temperatures longitudinally and transversely; the temperature of the transversal motion can be up to 10^3 times greater than the temperature of the longitudinal motion.

(d) From a thermodynamical point of view, the state of a typical ion beam is far from equilibrium and we must take into account that the cooling of the ion beam by an electron (or laser) cooler is accompanied by the heating of the beam due to intrabeam scattering (transfer of temperature from the transverse to the longitudinal direction), which increases with the density of the beam and the charge state of the ion.

We start with the case of an N-ionic periodic lattice with interionic distance d in equilibrium and circumference $L=Nd$. Our treatment is based on the harmonic approximation. In this case we can use the phonon formalism for the description of the ion chain. This approximation is valid if the temperature of the beam is small enough. Computer simulations of 3D Coulomb crystals [20,21] show that solid-liquid phase transition occurs at $\Gamma \approx 10^2$. In the case of a one-dimensional (1D) crystal there is no sharp phase transition [22], but we can expect that some crystal-like structures exist at $\Gamma > 10^2$. In Sec. II the basic principles of longitudinal Schottky diagnostics are considered and the relationship between a signal in the pick-up and the dynamical structure factor of a 1D crystal is obtained. In Sec. III we calculate the dynamical structure factor and consequently the Schottky spectrum of an ideal harmonic chain of ions. In Sec. IV we study the ion chain that interacts with a thermal bath, and both cooling and heating processes modify the form of the dynamical structure factor of the beam. A general discussion of these questions is found in Sec. V. In the Appendix we introduce the phonon description of the dynamics of the 1D lattice.

II. LONGITUDINAL PICK-UP DIAGNOSTIC OF THE ION-BEAM SCHOTTKY SPECTRUM

In the pick-up (PU) system each ion produces a signal

$$j(t)=\kappa Z e v_0 \phi(z(t)+v_0 t) , \tag{2.1}$$

where Z is the ion charge, $z(t)$ is the ion coordinate in a system that moves with the mean velocity of the beam v_0 relative to the PU, $\phi(z)$ is the normalized sensitivity function of the PU (see Fig. 1) $\int \phi(z)dz = 1$, and κ is the sensitivity factor of the PU. The mean value $j(t)$ is $j_0=\kappa Z e v_0/L$. We can use j_0 to normalize the signal in the PU. A beam of N ions with the coordinates z_j produces a signal

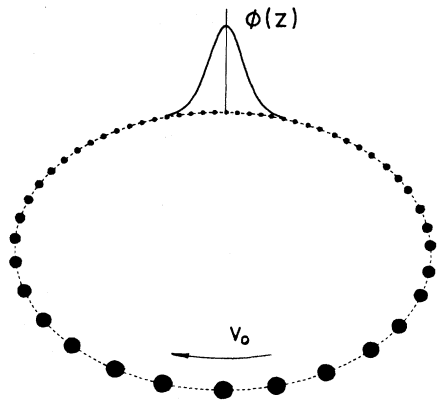

FIG. 1. Scheme of the pick-up diagnostics of the longitudinal Schottky spectrum in a storage ring. The ion beam moves with mean velocity v_0 relative to the PU. A profile of the sensitivity function of the PU is shown.

$$j(t)=j_0 L \sum_{j=1}^{N} \phi(z_j(t)+v_0 t) . \tag{2.2}$$

The periodicity of $\phi(z)$ in the case of a storage ring with circumference L gives us the possibility to express it as a Fourier series

$$\phi(z)=\sum_{M=-\infty}^{\infty} \phi_M \exp(-i2\pi M z/L) . \tag{2.3}$$

The Fourier transform over time of $j(t)$ is a sum of harmonics over M

$$J(\omega)=\sum_{M=-\infty}^{\infty} J_M(\omega - M\omega_0) , \tag{2.4}$$

where $\omega_0=2\pi v_0/L$ is the revolution frequency of the ion beam in a storage ring. The contribution from each harmonic in Eq. (2.4) is

$$J_M(\Omega)=j_0 L \phi_M \sum_{j=1}^{N} \int_{-\infty}^{\infty} e^{[i\Omega t - iQ_M z_j(t)]} dt , \tag{2.5}$$

where $\Omega=\omega - M\omega_0$ and $Q_M=2\pi M/L$ is the wave number of the Mth harmonic.

In Fig. 2 the Schottky spectra for the following three important special cases are shown (positive frequencies only).

(a) Ideal gas with $z_j(t)=z_j^0+v_j t$. The values z_j^0 are randomly distributed over the ring and the distribution of v_j corresponds to the Maxwellian distribution with temperature T and the average thermal velocity $v_{\rm th}=(2T/m)^{1/2}$,

$$J_M^{\rm IG}(\Omega)=2\pi j_0 L \phi_M \sum_{j=1}^{N} \delta(\Omega - Q_M v_j) e^{-iQ_M z_j^0} . \tag{2.6a}$$

The statistically averaged $|J(\omega)|$ is a superposition of Gaussian peaks $\sim \exp[-(\omega - M\omega_0)^2/(Q_M v_{\rm th})^2]$ located

near each harmonic of the revolution frequency of the beam ω_0. The width of the peaks increases with increasing M, and at large enough M these peaks overlap.

(b) At $T=0$ all $v_j=0$ and the ideal-gas limit yields

$$J_M^{\mathrm{IG}}(\Omega)=2\pi j_0 L\phi_M\delta(\Omega)\sum_{j=1}^{N}e^{-iQ_M z_j^0}. \tag{2.6b}$$

All peaks at $v_{\mathrm{th}}\to 0$ are transformed into δ functions; the intensity of each peak is of the order of $N^{1/2}$.

(c) Ideal 1D lattice at $T=0$ where $z_j(t)=jd$

$$J_M^{T=0}(\Omega)=2\pi\kappa Z e v_0\phi_M\delta(\Omega)\sum_{j=1}^{N}e^{-i2\pi M_j/N}$$

$$=2\pi j_0 L\phi_M\delta(\Omega)\delta_{M0}\,, \tag{2.6c}$$

where δ_{M0} is assumed to be over mod$N$. The spectrum contains only δ peaks at $\omega=0,N\omega_0,2N\omega_0,\ldots$; the intensity of each peak is proportional to N.

In a general case the procedure of a thermal averaging includes a calculation of the mean values over initial phase shifts for all collective modes and if $M\neq 0$ we obtain zero for the thermal average of $J_M(\omega)$. As we will see later if the frequency ω or the harmonic number M are small enough, the total spectrum $J(\omega)$ is the sum of nonoverlapping bands that corresponds to each value of M. In this case the square of $J(\omega)$ is also the sum of the squares of the contributions from the Mth band in Eq. (2.4),

$$\langle|J(\omega)|^2\rangle=\sum_M\langle|J_M(\Omega_M)|^2\rangle\,, \tag{2.7}$$

where $\Omega_M=\omega-M\omega_0$ and the contribution of the Mth harmonic is

$$\langle|J_M(\Omega_M)|^2\rangle=(j_0L\phi_M)^2\sum_{l,j=1}^{N}\left\langle\int\int e^{\{i\Omega_M(t_2-t_1)-iQ_M[z_j(t_2)-z_l(t_1)]\}}dt_1dt_2\right\rangle. \tag{2.8}$$

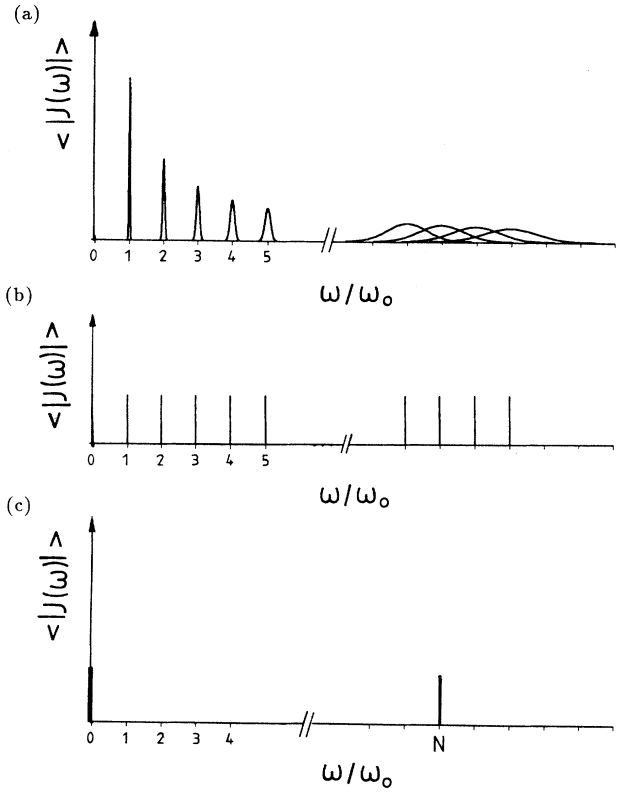

FIG. 2. The longitudinal Schottky spectrum of three ideal systems. The statistically averaged profile of $|J(\omega)|$ is plotted as a function of ω/ω_0. (a) Ideal gas at finite temperature; the spectrum is a superposition of Gaussian peaks located near each harmonic of the revolution frequency of the beam ω_0. The widths of peaks located near harmonic M increase with increasing M as $Q_M v_{\mathrm{th}}$ and at large enough M these peaks are overlapped. (b) Ideal gas at $T=0$; all peaks at $v_{\mathrm{th}}\to 0$ are transformed to δ functions, the intensity of each peak is of the order of $N^{1/2}$. (c) Ideal crystal at $T=0$; the spectrum contains only δ peaks at $\omega=0,N\omega_0,2N\omega_0,\ldots$; the intensity of each peak is proportional to N.

The function $\phi(z)$ is spread over some length D_{PU} that is of the order of the diameter of the PU. If the wavelength of the Mth Fourier harmonic $\lambda_M=2\pi M/L$ is much greater than D_{PU}, then we can use a δ-function approximation for the sensitivity function: $\phi(z)\approx\delta(z)$. In the rest of this paper we consider this case, which for usual pickups is valid for $M<10^4$, hence we have $\phi_M=1/L$. For higher harmonics the correct sensitivity function must be used in Eq. (2.8). The fact that the Mth band has no overlapping with other bands allows us to study the power spectrum of fluctuations in each band independently from other bands. In the rest of the paper we calculate the contribution of an isolated Mth band and can omit the index M in Q_M and Ω_M.

Equation (2.8) contains the density-correlation function of the ion beam [16,17]

$$I(Q,t_2-t_1)=\frac{1}{N}\sum_{l,j=1}^{N}\langle e^{-iQ[z_j(t_2)-z_l(t_1)]}\rangle\,, \tag{2.9}$$

which depends on the difference of t_2 and t_1 only. The Fourier transform of $I(Q,t)$ is expressed in terms of the dynamical structure factor of the chain

$$S(Q,\Omega)=\int_{-\infty}^{\infty}e^{i\Omega t}I(Q,t)\frac{dt}{2\pi}\,. \tag{2.10}$$

In an experiment the measurement of signals on a PU is performed over some finite time t_0. If we want to obtain the Schottky spectrum with resolution $\Delta\Omega$ we must take t_0 large enough so that $\Delta\Omega t_0\gg 1$. In this case an integration over both t_1 and t_2 in Eq. (2.8) from 0 to t_0 provides a direct relation between the Mth band of the Schottky power spectrum and the dynamical structure factor

$$\langle|J_M(\Omega)|^2\rangle=2\pi N j_0^2 t_0 S(Q,\Omega)\,. \tag{2.11}$$

The calculation of the dynamical structure factor of the ion beam in a storage ring is the main purpose of the present paper.

Our analysis of Schottky spectra was performed in a coordinate system moving with the ion beam. However, PU measurements are made in a laboratory system and in the case of a relativistic ion beam with $\gamma=[1-(v_0/c)^2]^{-1/2}$ we must transform the Schottky spectrum into a comoving system. Frequency Ω', time t_0', and current j_0' in a laboratory system are related to their values in a comoving system by $t_0=t_0'/\gamma$, $\Omega=\Omega'\gamma$, and $j_0=j_0'\gamma$. This provides

$$S(Q,\Omega)=\frac{\gamma\langle|J_M^2(\Omega/\gamma)|\rangle}{2\pi t_0' N|j_0'|^2} . \tag{2.12}$$

The total power of the Mth band of the Schottky spectrum is related to the static structure factor

$$S(Q)=\int_{-\infty}^{\infty} S(Q,\Omega)d\Omega=I(Q,0) . \tag{2.13}$$

III. HARMONIC DYNAMICS OF THE ION BEAM

At temperature $T=0$ the equilibrium structure of the one-dimensional lattice is an ideal linear chain with the average interionic distance $d=L/N$. The z coordinate of the jth ion is the sum of the position at equilibrium $z_j^0=dj$ and the displacement from the equilibrium $u_j(t)$,

$$z_j(t)=dj+u_j(t) \quad (j=1,\ldots,N) . \tag{3.1}$$

The phonon amplitude $a(q)=a(q,t)$ is determined as a Fourier transform of the ionic displacements

$$a(q)=\frac{1}{\sqrt{N}}\sum_{j=1}^{N} u_j e^{-iqdj} \text{ for each } q=\frac{2\pi}{L}k . \tag{3.2}$$

In a coordinate system moving with the ion beam $a(q=0)=0$.

The interaction between ions in a storage ring is described by a modified Coulomb potential $U(z)$. The short-range modification is related to the influence of a finite amplitude of transversal oscillations $a_\perp$ [see Fig. 3 and Eq. (A8) in the Appendix]. The long-range modification is the effective screening by the charge induced on the metallic tube of a storage ring. In the rest of this paper we use the harmonic approximation that corresponds to neglecting in the expansion of the potential energy all terms higher than $u_j u_l$. This limits the validity of our model to sufficiently small longitudinal temperature ($\Gamma>1$).

In the case of an ideal phonon system we can use the phonon formalism to calculate some thermally averaged characteristics of the ion beam. In accordance with the Boltzmann formula, the probability of observing the ionic configuration with the potential energy Φ is proportional to $\exp(-\Phi/T)$. We note that in the presence of dissipation the Boltzmann distribution ansatz is no longer justified in general as will be seen later. The use of the basis of phonon amplitudes is preferable because on this basis the total potential energy is a simple sum of terms, each related to a single q and there are no terms containing the product of phonon amplitudes with distinct q. On the basis of phonon amplitudes $\exp(-\Phi/T)$ is a product of multiples, each of which depends on a single-phonon amplitude $a(q)$. This fact allows us to calculate the mean

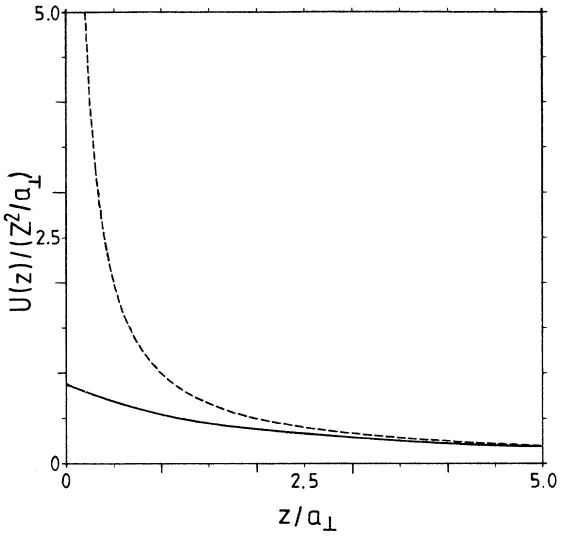

FIG. 3. The potential of interaction (in units of $(eZ)^2/a_\perp$) of two charged disks (solid line) and two charged points (dashed line) as a function of the distance z between them.

values for each phonon mode independently from another. Each phonon mode is a harmonic oscillator with the potential energy $m\omega^2(q)a^2(q)/2$. The phonon frequency $\omega(d)$ for an ion chain in a storage ring is calculated in the Appendix (see Fig. 4).

The mean square of the phonon amplitude is [16]

$$\langle|a(q,t)|^2\rangle=\frac{T}{m\omega^2(q)} . \tag{3.3}$$

In the state of the thermodynamic equilibrium the temperature T is a constant; but in our case the mean kinetic energy and amplitude of each phonon mode are deter-

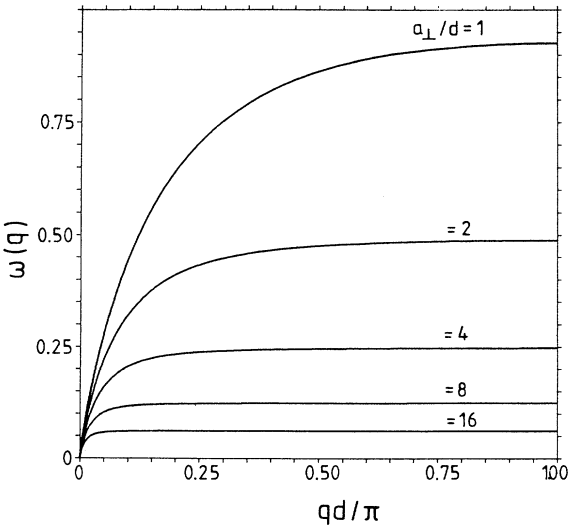

FIG. 4. Typical longitudinal phonon spectra $\omega(q)$ [in units of $Z/(md^3)^{1/2}$] of the 1D Coulomb crystal for some values of the amplitude of transversal oscillations $a_\perp$. All curves are calculated for the ratio of the interionic spacing to the radius of effective screening of the Coulomb interaction $d/D=10^{-3}$.

mined as a result of the competition between cooling and heating of the beam (see Fig. 5). Now the temperature can be a function of q, and we can use Eq. (3.3) as a definition of $T(q)$. The function $T(q)$ then is determined by the cooling and heating rates $\nu_c(q)$ and $\nu_h(q)$.

The phonon frequency $w_k=\omega(q)$ tends to zero at small q as

$$\omega(q)\approx c_s|q| \ , \tag{3.4}$$

where c_s is the sound velocity of the ionic chain

$$mc_s^2=2[(eZ)^2/d]\Lambda \ , \tag{3.5}$$

with Λ the logarithm of the ratio of the screening length D to the interionic distance d or to the amplitude of transversal oscillations $a_\perp$ if $a_\perp > d$ (see the Appendix). In any case typical values of Λ do not exceed 10. From Eq. (3.3) it follows that in thermal equilibrium the maximum of the phonon amplitude corresponds to the phonons with smallest q.

The ratio of the mean amplitude of thermal oscillations to the interionic distance is called the Lindemann ratio C_L [23]. Using Eq. (3.3) we obtain, for the case of T independent of q,

$$C_L^2=\frac{\langle|u_l(t)|^2\rangle}{d^2}=\frac{T}{md^2N}\sum_q\frac{1}{\omega^2(q)} \ . \tag{3.6}$$

In the case of an infinite chain the sum over q must be replaced by an integral. The acoustic behavior of phonon frequency at small q results in an infinite value for $\langle|u_l(t)|^2\rangle$. The infinite amplitude of thermal oscillations of all ions is a typical property of 1D (and also 2D) crystals. In 3D crystals there also exist acoustic phonons with $\omega(\mathbf{q})\approx c_s|\mathbf{q}|$, but the integral like Eq. (3.6) over d^3q has no divergence at small q and the mean square of atomic displacements has a finite value. This means that in 3D crystals there exists long-range order, but in 1D crystals there exists only short-range order.

In the case of a larger, but finite N we can extract the divergent term in Eq. (3.6). At small q we can use the long-wavelength approximation for the phonon frequency (3.4). It provides

$$C_L^2\approx\frac{2NT}{mc_s^2(2\pi)^2}\sum_{k=1}^{\infty}\frac{1}{k^2}=\frac{N}{24\Gamma\Lambda} \ . \tag{3.7}$$

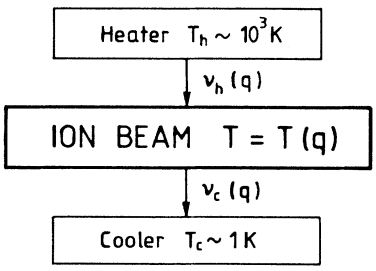

FIG. 5. The illustration of the thermal flow at a nonequilibrium state. The mean kinetic energy of each phonon mode is a result of steady-state equilibrium between heating and cooling; the rates of two these processes are q dependent and the phonon temperature is also a function of q.

Analysis of experimental data concerning solid-liquid phase transition [23,24] yields an empirical criterion for the melting temperature of 3D crystals: this phase transition takes place at $C_L\approx 0.1$. Molecular-dynamics simulation of 3D Coulomb systems [20,21] shows that solid-liquid transition occurs at $\Gamma\approx 170$. The same value of Γ in the case of a 1D ion beam with $N\sim 10^6$ particles implies a Lindemann ratio of the order of 10^1 or the mean amplitude of thermal oscillations is much greater than the interionic spacing d.

To test the validity of using the harmonic approximation if $\Gamma>1$ but C_L is also greater than unity we must calculate the spatial correlation function. In the framework of the long-wavelength approximation (3.4) from Eq. (3.3) follows

$$\begin{aligned}\langle[u_{l+j}(t)-u_l(t)]^2\rangle/d^2 &=\frac{2}{Nd^2}\sum_q\langle|a(q,t)|^2\rangle[1-\cos(qdj)] \\ &=\frac{N}{\pi^2 2\Gamma\Lambda}G(2\pi j/N) \ ,\end{aligned} \tag{3.8}$$

with [25]

$$G(w)=\sum_{k=1}^{\infty}\frac{1-\cos(kw)}{k^2}=\frac{(2\pi-w')w'}{4}$$

$$\text{where } w'=w \bmod 2\pi \ . \tag{3.9}$$

Analysis of the correlations of ionic displacements in Eq. (3.8) shows that at $\Gamma\gg 1$ the relative displacements of neighboring ions are much smaller than d and this justifies the use of the harmonic approximation in spite of the large amplitude of ionic oscillations ($C_L>1$).

The phonon formalism allows us to calculate the two-time correlators,

$$\begin{aligned}W_j(t)&=\langle[u_{l+j}(t+t')-u_l(t')]^2\rangle \\ &=\frac{2}{N}\sum_q(1-e^{-idqj})\langle a^*(q,t+t')a(q,t')\rangle \ .\end{aligned} \tag{3.10}$$

For an ideal harmonic oscillator [16]

$$\langle a^*(q,t+t')a(q,t')\rangle=\frac{T\cos[\omega(q)t]}{m\omega^2(q)} \ . \tag{3.11}$$

In the frame of the long-wave approximation (3.4)

$$W_j(t)=\frac{dL}{4\pi^2\Lambda\Gamma}\left[G\left[\frac{2\pi(jd-c_st)}{L}\right]+G\left[\frac{2\pi(jd+c_st)}{L}\right]\right] \ . \tag{3.12}$$

To obtain the mean value of $\exp\{-iQdj-iQ[u_{j+l}(t+t')-u_l(t')]\}$ in Eq. (2.9) we can perform independent thermal averaging of each phonon mode q.

This gives

$$\langle e^{-iQ[u_{j+l}(t+t')-u_l(t')]}\rangle = e^{-Q^2W_j(t)/2} . \quad (3.13)$$

In the case $\Gamma \gg 1$ the exponent in Eq. (3.13) is a slowly varying function of j. This means that we can replace the discrete function $W_j(t)$ by the continuous function of $z=dj$ and replace the summation over j by integration over z. As we can see in Eq. (3.12) for $L \gg d$ the main contribution to the function $W(z,t)$ is obtained by using the long-wave approximation. Taking into account dispersion produces only a small correction to it. The dynamical structure factor (2.12) is the two-dimensional Fourier transform of $\exp[-Q^2W_j(t)/2]$ and now we must analyze the properties

$$\exp[-Q^2W(z,t)/2] = \exp\left\{-\alpha^2\left[G\left[\frac{2\pi(z-c_st)}{L}\right]+G\left[\frac{2\pi(z+c_st)}{L}\right]\right]\right\} , \quad (3.14)$$

where $\alpha^2=M^2/(2\Gamma\Lambda N)$.

The function $\exp[-\alpha^2G(w)]$ is a periodical function of w with period 2π. Its Fourier transform is expressed in terms of the complex error function [26]

$$H(k)=\frac{1}{2\pi}\int_0^{2\pi} e^{[ipw-\alpha^2G(v)]}dw = \frac{i}{2\sqrt{\pi}\alpha}e^{(-k/\alpha+i\pi\alpha/2)^2} \times[\mathrm{erf}(k/\alpha-i\alpha\pi/2)-\mathrm{erf}(k/\alpha+i\alpha\pi/2)] . \quad (3.15)$$

Substituting (3.14) into Eqs. (2.10), (2.9), performing integration over t and z, and using orthogonality relations for the Fourier transform, we obtain

$$S(Q,\Omega)=\sum_{k=-\infty}^{\infty} B_k\delta(\Omega-k\Omega_s) , \quad (3.16)$$

where $\Omega_s=2\pi c_s/L$ is the revolution frequency of a sound wave in the storage ring,

$$B_k=NH\left[\frac{M-k}{2}\right]H\left[\frac{M+k}{2}\right]$$

if $M\pm k$ are even numbers (3.17)

and $B_k=0$ if $M\pm k$ are odd numbers.

The dynamical structure factor $S(Q,\Omega)$ is a sum of δ functions, but an experimental measurement of $\langle|J(\Omega)|^2\rangle$ transforms each δ function into a band with the characteristic width of the order t_0^{-1}.

As we will discuss below the δ-function structure of $S(Q,\Omega)$ exists if the characteristic cooling and heating time scales are long compared with the time scale of the measurement. This δ-function structure of the dynamical structure factor is a consequence of the space-time periodicity of correlation functions (see Fig. 6). If we produce some distortion of density of the beam at time $t=0$, it provides two waves moving with velocity c_s to the left and to the right on the ring. At time $t_s=L/c_s$ both of these waves come back to the initial point and we obtain the same density profile as at $t=0$. Moreover, as we can see from Fig. 6(c) there exists also a combined type of symmetry. At time $t=t_s/2$ when all excitations are passing only half of the ring, they also recombine into their initial state, but rotated by 180° (or shifted on $L/2$). This explains why only odd or only even B_k are not equal to zero in Eq. (3.17) and the distance between δ peaks is $2\Omega_s$.

Typical profiles of the dynamical structure factor are presented in Fig. 7. In the case $\alpha \gg 1$ from (3.15) it follows [18] [see Fig. 7(a)]

$$H(k)=\frac{\alpha^2/4}{(\pi\alpha^2/4)^2+k^2} . \quad (3.18)$$

This case is typical for the case of neutron spectroscopy of phonons in quasi-one-dimensional crystals [19] where $L\to\infty$ but the wave vector Q has some fixed value so that the harmonic number $M=LQ/(2\pi)$ also tends to infinity. The interval between δ peaks $2\Omega_s$ tends to zero and the fine structure of the spectrum is smoothed. The dynamical structure factor (3.16) is a product of two Lorentzian functions (3.18) and the width of each

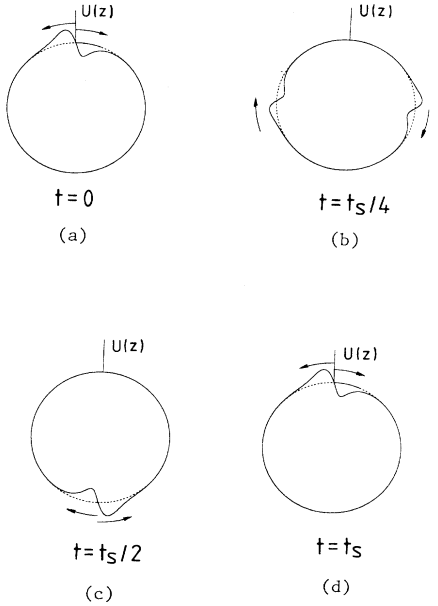

FIG. 6. Propagation of long-wave excitation in a cyclic 1D crystal with no dissipation. The profile of an ionic displacement $u_j(t)=u(z)$ is shown for (a) $t=0$, some initial profile of displacements (and velocities) is excited; (b) at $t>0$ these initial excitations produce two waves moving in opposite directions in a storage ring; (c) at $t=t_s/2$ these two waves result in the initial profile but rotated by 180°; (d) at $t=t_s$ the system returns to the initial state.

Lorentzian function is proportional to the temperature.

In the opposite limiting case $\alpha \ll 1$ we can expand (3.17) in a power series in α^2 (or temperature)

$$H(k)=\alpha^2/(2k^2) \quad \text{at } k\neq 0 , \tag{3.19}$$

$$H(0)=1-\alpha^2\pi/12 \quad \text{at } k=0 . \tag{3.20}$$

The dynamical structure factor has the structure shown in Fig. 7(b). At $\Omega=\pm c_s Q$ there are two peaks with the intensity proportional to the first power of temperature,

$$B_{\pm M}\approx\frac{L\alpha^2}{2M^2}=\frac{1}{2\Gamma\Lambda} . \tag{3.21}$$

The intensity of all other peaks is a product of two H_k with $k\neq 0$ and contains a fourth power of α or a square of the temperature.

IV. THE DYNAMICAL STRUCTURE FACTOR OF AN ION BEAM WITH DISSIPATION

In the general case our ion beam is not an isolated system but rather interacts with cooling and heating baths

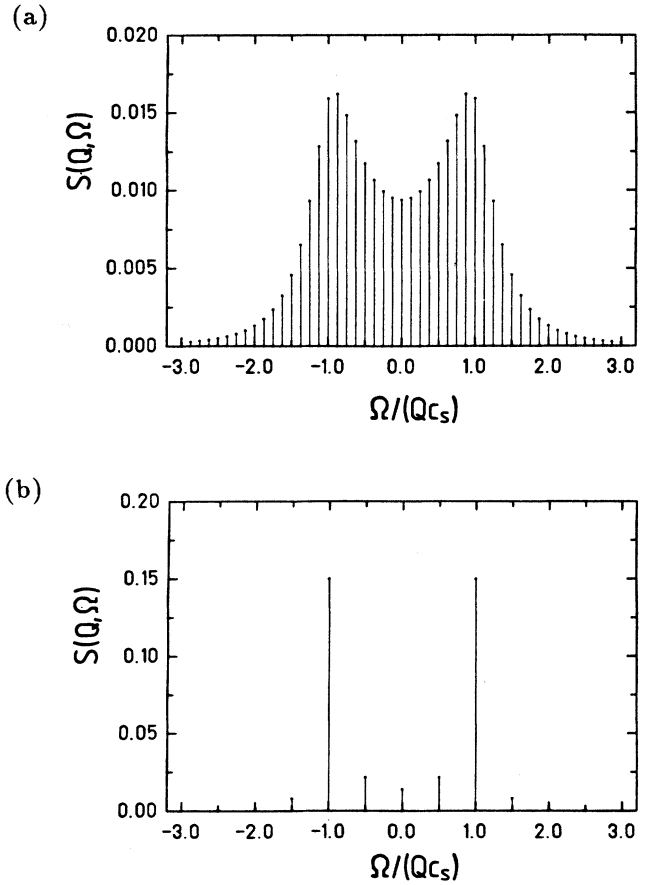

FIG. 7. Typical plots of the dynamical structure factor of a 1D ordered beam in a storage ring without dissipation. Profiles have a δ-peak structure with spacing $2\Omega_s$ between peaks: (a) in the high-temperature case with $M=16$, $\alpha=1.6$ the envelope curve of δ peaks is a product of two Lorentzians; (b) in the low-temperature case $M=4$, $\alpha=0.4$ there are two main peaks at $\Omega=\pm\omega(Q)$.

through rates $\nu_c(q)$ and $\nu_h(q)$. The form of the function $\nu_c(q)$ depends on the details of the electron-cooling friction force. The longitudinal heating is a result of collisions of the ions, which are supposed to have a transverse temperature (emittance). This well-known intrabeam scattering depends on the local values of the density and the temperatures. These vary around the ring according to the focusing structure of a particular storage ring, and a calculation of rates requires a considerable numerical effort [27]. In the remainder of this paper we make the simplifying assumption that the (longitudinal) temperature as well as the cooling rate are independent of q. The equilibrium can thus be described by two parameters T and ν, where the latter is the effective relaxation rate. The interaction with the thermal bath provides some fluctuations of the energy of the beam and we can take into account that this interaction modifies the phonon equations of motion. If we assume that the ion beam is a part of a big harmonic system then we can use Eq. (3.13) to calculate the dynamical structure factor. In calculating $W_j(t)$ we must take into account the influence of the interaction with the whole system (thermal bath). The standard procedure is to use the phonon equations of motion under the action of a random heating force $F(t)=my(t)$ and a viscosity term that describes the interaction with the cooling system

$$\ddot{a}(q,t)+\nu\dot{a}(q,t)+\omega^2(q)a(q,t)=y(t) . \tag{4.1}$$

In the case with no time correlations of $y(t)$ ("white noise," see Ref. [22]) we can allow the statistically averaged values of $\langle |Y(\omega)|^2\rangle$ to be equal to some constant that is proportional to the temperature of the thermal bath. This implies

$$\langle a^*(q,t+t')a(q,t')\rangle = \frac{\nu T}{\pi m}\int_{-\infty}^{+\infty}\frac{\exp(i\omega t)d\omega}{[\omega^2-\omega^2(q)]^2+\nu^2\omega^2} . \tag{4.2}$$

The value of the prefactor in (4.2) is determined from Eq. (3.3) for the mean potential energy at the state of thermal equilibrium.

Now we can calculate $W_j(t)$. From (3.10) it follows

$$W_j(t)=\sum_q \frac{2T(q)\nu(q)}{m\pi N} \times\int_{-\infty}^{+\infty}\frac{1-\exp[i(\omega t-qdj)]}{[\omega^2-\omega^2(q)]^2+\nu^2(q)\omega^2}d\omega . \tag{4.3}$$

This equation takes into account that both the temperature and the relaxation rate may depend on q.

The dynamical structure factor is the two-dimensional Fourier transform of $\exp[-Q^2W_j(t)]$ and now we must analyze the properties of $W_j(t)$ as a function of j and t. As we can see in Sec. III the collective motion of ions in a 1D lattice is well correlated at a small distance dj between l and $l+j$ ions [$W_0(t=0)=0$]. The function $W_j(t=0)$ increases with increasing j and reaches the maximum value $W_{\max}$ at $j=N/2$ and then decreases so that $W_N(t=0)=0$. From (3.14) it follows that

$W_{\max} < 4d^2 C_L^2$ or

$$Q^2 W_{\max} < \frac{2\pi^2 M^2}{3\Gamma\Lambda N} . \tag{4.4}$$

$W_j(t)$ has the same properties as a function of time in the case with no dissipation and dispersion: the function $W_j(t)$ is symmetric relative to the change $jd \to c_s t$ in Eq. (3.12) and this function is a periodic function of t with the period $t_s = L/c_s$ (see both dashed curves in Fig. 8).

In the case of finite relaxation rate ν the periodicity of $W_j(t)$ over t is broken (see Fig. 8) and at $t > \nu^{-1}$ the function $W_j(t)$ tends to $W_{\max}$. For the PU diagnostic it is important to consider a case of small enough M so that $Q^2 W_{\max} \ll 1$. This requires $M^2 \ll 3\Gamma\Lambda N/(2\pi^2)$ or $\alpha \ll 1$, where α was determined in Eq. (3.14). We simply denote this case as the low-temperature case, where α also depends on both T and M. In this case we can expand the exponent in Eq. (3.13) into a power series in $Q^2 W_j(t)$ and take the linear term only. This gives

$$S(Q,\Omega) = \left[\frac{(Qc_s)^2}{2\pi\Lambda\Gamma(Q)} \right] \frac{\nu(Q)}{[\Omega^2 - \omega^2(Q)]^2 + \nu^2(Q)\Omega^2} . \tag{4.5}$$

The plots of the dynamical structure factor for this case of small α are shown in Figs. 9(a) and 9(b) for some values of ν. In the case of $\nu \ll \omega(Q)$ the profile has two

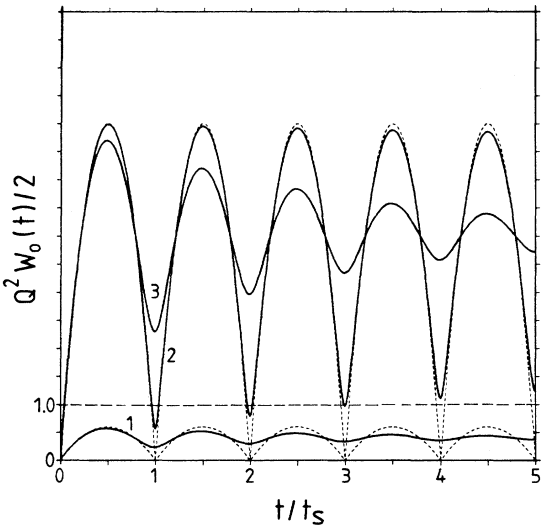

FIG. 8. Schematic plot of the function $W_0(t)$ for some values of temperature and relaxation frequency ν. In the low-temperature case $\alpha \ll 1$ (curve 1) we have $Q^2 W_{\max} < 1$ and all t (and z) give an appreciable contribution to $S(Q,\Omega)$; at $\nu = 0$ (dashed line) the periodicity of $W_0(t)$ results in a δ-peak structure of $S(Q,\Omega)$; in the high-temperature case $\alpha \gg 1$ with small enough ν it is important that at $t = t_s, 2t_s, 3t_s, \ldots$ (curve 2) up to some multiple n_ν of the period of sound-wave revolution, where $Q^2 W_0(t)/2$ is of the order or smaller than 1. The spectrum has the fine structure like in Fig. 7(b) but the widths of the peaks are of the order of Ω_s/n_ν [the profile of $W_0(t)$ for the case $\nu = 0$ is shown as a dashed line]. At large enough ν (curve 3) only a small interval of time $|t| < t_Q$ is important for calculating the dynamical structure factor.

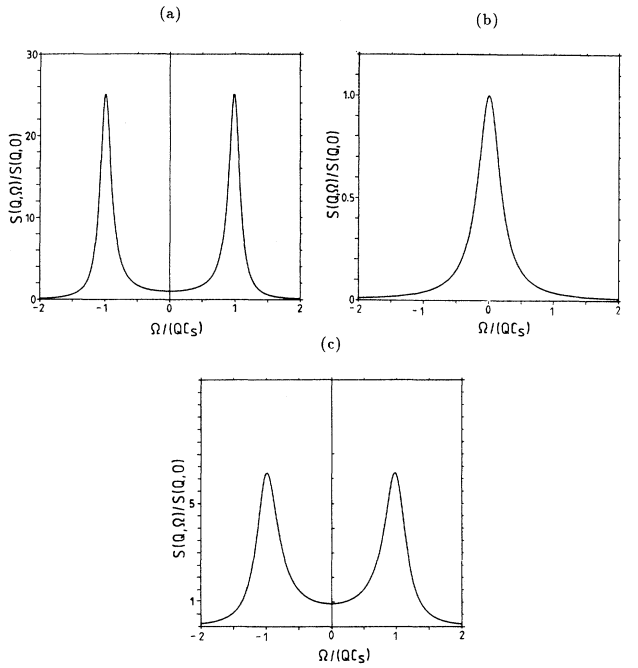

FIG. 9. Plots of the dynamical structure factor $S(Q,\Omega)$, parameters $S(Q,0)$, $S_{\max}$, and $\delta\omega$ are listed in Table III for some values of T, M, and ν: (a) at $\alpha \ll 1$ and $\nu \ll Qc_s$ there are two well-distinguished peaks located at $\Omega = \pm Qc_s$ with the widths of the order of ν; (b) at $\alpha \ll 1$ but $\nu \gg Qc_s$ there is only a central peak with the width $\delta\omega \approx Q^2 c_s^2/\nu$; (c) in the high-temperature case ($\alpha \gg 1$) the width γ_Q of two peaks located at $\Omega = \pm Qc_s$ does not depend on ν.

well-distinguished peaks at $\Omega = \pm\omega(Q)$ with the width of the order of ν. If $\nu \gg \omega(Q)$ then the profile has a central diffuse peak. The total power of the Mth band of the Schottky spectrum is related to the static structure factor (2.13)

$$S(Q) = Q^2 \langle |a(Q,t)|^2 \rangle = \frac{1}{2\Gamma(Q)\Lambda} , \tag{4.6}$$

where we have taken into account that Γ may be a function of Q. The static structure factor is independent of ν and may be used for a direct measurement of the temperature distribution function $T(Q)$. The information on the relaxation frequency is available from the width of the peaks of $S(Q,\Omega)$ in Fig. 9.

In the opposite "high-temperature" case, $\alpha \gg 1$, and contributions of all phonon modes into $S(Q,\Omega)$ are mixed. Typical plots of $W_0(t)$ as a function of time for this case are shown in Fig. 8 (curves 2 and 3). In the case of a small relaxation rate ($t_s \nu \ll 1$) the profile of $W_j(t)$ at times of a few periods of the revolution of a sound wave in a storage ring t_s is similar to the $W_j(t)$ in the case of no dissipation and the profile of the dynamical structure factor corresponds to Fig. 7, but in this case all δ functions are spread into the peaks with the characteristic width of the order of ν. We can introduce some characteristic time of fluctuation decay t_Q that corresponds to $Q^2 W_0(t_Q)/2 = 1$. In the Fourier transform (3.19) only the interval of $|t| \sim t_Q$ is important. In this case the

TABLE I. Parameters for ESR storage ring.

		Laboratory system	Comoving system
Ions		$_{238}U^{92+}$	
Ion kinetic energy	E_i	500 MeV/u	
Relativistic factor	γ_i	1.537	
Number of ions	N	1.0×10^{6}	
Circumference	L	1.09×10^{4} cm	0.71×10^{4} cm
Interionic distance	d	0.71×10^{-2} cm	
Ion velocity	v_0	2.27×10^{10} cm/s	
Current per ion	j_0	4.7×10^{-11} A	3.1×10^{-11} A
Transverse amplitude	$a_\perp$	0.05 cm	
Logarithmic factor	Λ	5.3	
Sound velocity	c_s	0.86×10^{5} cm/s	
	Frequencies of revolution		
Ion beam	ω_0	1.3×10^{7} s^{-1}	2.0×10^{7} s^{-1}
Sound wave	Ω_s	50 s^{-1}	76 s^{-1}

dynamical structure factor corresponds to the case of an infinite chain of atoms. If $vt_c \ll 1$ we need also not take into account the dissipation. The long-wave approximation (3.16) with $G(w)\approx\pi|w|/2$ at small w provides

$$W_j(t)\approx\frac{d}{4\Lambda\Gamma}(|jd-c_st|+|jd+c_st|)\ . \tag{4.7}$$

It provides $t_Q=4\Lambda\Gamma/(dc_sQ^2)$. The dynamical structure factor is [18]

$$S(Q,\Omega)=\frac{4c_s}{\pi d}\frac{\gamma_Q^2}{[\gamma_Q^2+(c_sQ+\Omega)^2][\gamma_Q^2+(c_sQ-\Omega)^2]}\ , \tag{4.8}$$

where $\gamma_Q=1/t_q$. A typical plot of $S(Q,\Omega)$ for this case is presented in Fig. 9(c). The profile of the dynamical structure factor has two well-distinguished peaks at $\Omega=\pm c_sQ$ with width γ_Q [the ratio of γ to Qc_s is equal to $(Qd)/(4\Lambda\Gamma)\ll1$]. In the case of large relaxation rate $\nu>\gamma_Q$ the width of these peaks is of the order of ν.

It is important that the long-wave approximation for $W_j(t)$ is possible at large enough j and t only. The phonon dispersion is important if the phonon wavelength is smaller than the effective radius of interionic interaction D (see the Appendix). This means that Eqs. (3.12) and (4.7) can be used only outside small regions $|jd|<D$ and $|tc_s|<D$. In the low-temperature case these regions give only a small contribution to the dynamical structure factor in Eq. (4.5). But in the case of very large α^2 the main contribution to (4.8) provides a small interval of t and z, and the long-wave approximation (4.7) is not enough. Some questions concerning numerical computation of $S(Q,\Omega)$ for 1D phonons with dispersion are analyzed in Ref. [19].

V. GENERAL DISCUSSION

Now we try to use our theory to describe possible Schottky spectra. As an example, in Table I there are listed some parameters of a $_{238}U^{92+}$ ion beam for the ESR storage ring at GSI Darmstadt. The values of the parameter Γ and the relative momentum spread $\delta p/p=(T/mv_0^2\gamma_i^2)^{1/2}$ as a function of T are listed in Table II. Our harmonic approximation is possible at $\Gamma\gg1$ or at $T\ll2\times10^3$ K. In this table is also given the static structure factor $S(Q)$. In the framework of our harmonic approximation the value of $S(Q)$ is proportional to T and independent of M (and ν). The parameter α is calculated for M up to 10^4. For higher M we must take into account the spread of the sensitivity function $\phi(z)$ in Eq. (2.8). We can see that the "low-temperature" case $\alpha<1$ applies for all T and M except in the limit of very large T and M.

In Table III are listed parameters of the profiles of the dynamical structure factor in Fig. 9 for some T, M, and ν. In the low-temperature case at $T<1000$ K at $Qc_s<\nu$ there are two peaks at $\Omega=\pm Qc_s$ with the width of the order of ν [Fig. 9(a)]. At $Qc_s>\nu$ there is a single peak with

TABLE II. Parameters of the ion beam.

				α		
T (K)	Γ	$\delta p/p$	$S(Q)$	($M=1$)	($M=10^2$)	($M=10^4$)
0.1	2×10^4	0.82×10^{-7}	0.47×10^{-5}	0.22×10^{-5}	0.22×10^{-3}	0.22×10^{-1}
1	2×10^3	2.6×10^{-7}	0.47×10^{-4}	0.69×10^{-5}	0.69×10^{-3}	0.69×10^{-1}
10	2×10^2	0.82×10^{-6}	0.47×10^{-3}	0.22×10^{-4}	0.22×10^{-2}	0.22
100	2×10^1	2.6×10^{-6}	0.47×10^{-2}	0.69×10^{-4}	0.69×10^{-2}	0.69
1000	2	0.82×10^{-5}	0.47×10^{-1}	0.22×10^{-3}	0.22×10^{-1}	2.2

TABLE III. Parameters of the dynamical structure factor.

	ν [s^{-1}]	Qc_s [s^{-1}]	$S(Q,0)$ [s]	S_{max} [s]	$\delta\omega$ [s^{-1}]	Fig.
$T=1$ K						
$M=1$						
	1	0.76×10^{2}	0.26×10^{-9}	0.15×10^{-5}	$=\nu$	9(a)
	10^{2}	0.76×10^{2}	0.26×10^{-7}	$=S(Q,0)$	0.58×10^{2}	9(b)
	10^{4}	0.76×10^{2}	0.26×10^{-5}	$=S(Q,0)$	0.58	9(b)
$M=100$						
	1	0.76×10^{4}	0.26×10^{-13}	0.15×10^{-5}	$=\nu$	9(a)
	10^{2}	0.76×10^{4}	0.26×10^{-11}	0.15×10^{-7}	$=\nu$	9(a)
	10^{4}	0.76×10^{4}	0.26×10^{-9}	$=S(Q,0)$	0.58×10^{4}	9(b)
$M=10^{4}$						
	1	0.76×10^{6}	0.26×10^{-17}	0.15×10^{-5}	$=\nu$	9(a)
	10^{2}	0.76×10^{6}	0.26×10^{-15}	0.15×10^{-7}	$=\nu$	9(a)
	10^{4}	0.76×10^{6}	0.26×10^{-13}	0.15×10^{-9}	$=\nu$	9(a)
		...	...	...	...	
T		$\times1$	$\times T$	$\times T$	$\times1$	
		...	...	...	...	
$T=10^{3}$ K						
$M=10^{4}$						
	$\nu<10^{3}$	0.76×10^{6}	0.15×10^{-10}	0.17×10^{-5}	0.11×10^{4}	9(c)

the width $\delta\omega=(Qc_s)^2/\nu$ [Fig. 9(b)]. An increase of temperature produces a proportional increase of the values of $S(Q,0)=S(Q,\omega=0)$ and S_{max}. The width of the peaks is independent of T. It is important to note that in the low-temperature case both static and dynamical structure factors give information concerning the temperature and ν for each phonon mode.

In the "high-temperature" case [$T=1000$ K, $M=10^4$, see Eq. (4.8) and the last line in Table III] the width of the two peaks in Fig. 9(c), $\delta\omega=\gamma_Q$, is proportional to T and independent of ν for $\nu\ll\gamma_Q$. In this case all contributions of phonon modes into $S(Q,\Omega)$ are mixed and the Schottky spectrum gives information concerning some average phonon temperature of the beam.

It is interesting to compare the Schottky spectrum of a strongly correlated phonon system with the case of the ideal gas in Eq. (2.6a). Each band of the spectrum of the harmonic system has a width of the order of $2Qc_s$, whereas the width of peaks in the case of an ideal gas is of the order of $2Qv_{th}$. From Eq. (3.5) it follows that $v_{th}^2/c_s^2=1/(\Gamma\Lambda)$ and in our case $\Gamma>1$ we have $v_{th}\ll c_s$. For a system with $\Gamma>1$ and not too large M (i.e., $\alpha\ll1$) the form of the Schottky spectrum depends on M, if the cooling rate is large enough. A single-peaked spectrum at low M is changing into a double-peaked spectrum at a sufficiently large M. This is opposed to the ideal-gas case, where one expects that the two peaks merge into one peak due to a reduction of c_s for short wavelength. It is proposed that this dependence on M can be used in the experiment as a signature of correlations or ordering.

ACKNOWLEDGMENTS

The authors thank R. W. Hasse and R. Maier for helpful discussions. One of the authors (V.V.A.) expresses his gratitude for the hospitality of GSI Darmstadt.

APPENDIX: HARMONIC PHONONS IN A TWO-TEMPERATURE 1D COULOMB LATTICE

The phonon frequency $\omega(q)$ is determined by

$$\omega^2(q)=\frac{1}{m}\sum_{l=-\infty}^{\infty}\left[1-\cos\left[\frac{qdl}{N}\right]\right]U''(dl)\ . \tag{A1}$$

In the case of a small transverse temperature $a_\perp\ll d$ and the potential of the interionic interaction is approximately of the Coulomb type: $U=Z/|z|$ and

$$\omega^2(q)=\frac{4(eZ)^2}{md}\sum_{l=1}^{\infty}\frac{1-\cos(qdl)}{l^3}\ . \tag{A2}$$

In the limit of small q it provides

$$\omega^2(q)\approx\frac{2(eZ)^2}{md}q^2|\ln|qd||\ . \tag{A3}$$

This nonanalytic behavior of the phonon frequency at small q is a consequence of the long-range character of the Coulomb interaction. If we try to calculate the sound velocity

$$c_s=\lim_{q\to0}\omega(q)/q\ , \tag{A4}$$

then the sum on l diverges or the sound velocity of the infinite chain with Coulomb interaction tends to infinity.

A first modification of the interaction potential is the effective screening of the Coulomb interaction by the charges induced on the metallic vacuum chamber of a storage ring. For a perfectly conducting wall all field lines are perpendicular to the wall, which limits the interaction to a maximum screening length D of the order of the diameter of the vacuum chamber. In calculating the phonon frequency and the sound velocity we must truncate the interionic interaction at distances larger than D or introduce in Eq. (A1) some screening factor

that vanishes at distances greater than D. If we take this screening factor as $\exp(-z/D)$ it provides

$$\frac{d^2\omega^2(q)}{dq^2}=\frac{4(eZ)^2}{md}\sum_{l=1}^{\infty}\cos(qld)\exp(-ld/D)$$
$$=-\frac{4(eZ)^2}{md}\ln|1-e^{(iqd-d/D)}| . \quad \text{(A5)}$$

Equation (A5), in the limiting case $q \gg D^{-1}$, transforms into Eq. (A2) but in the long-wave limit $q \ll D^{-1}$ it provides a soundlike dispersion law $\omega(q)\approx c_s|q|$ with

$$c_s^2=\frac{2(eZ)^2}{md}\ln(D/d) . \quad \text{(A6)}$$

The finite amplitude of transversal thermal oscillations also modifies the potential of the interionic interaction at distances of the order of $a_\perp$. From the dynamics of electron and laser cooling of the ion beam it is more obvious to expect extremely low longitudinal temperatures, whereas the transverse might be much higher. It is also important that the transverse oscillation frequencies are much larger than the phonon frequency of the longitudinal motion. This rather anharmonic system may be described within the method of self-consistent phonon approximation [28]. In the description of a slow system (longitudinal phonons) we can use the potential averaged over the motion of a fast subsystem (transversal motion). The transversal focusing potential of the ion beam $U_b(r)=m\omega_b^2 r^2/2$ is characterized by the betatron frequency ω_b, which is assumed to be independent of the longitudinal coordinate z. The distribution of radial charge density can be assumed to be a Boltzmann distribution with the transverse temperature $T_\perp$. For sufficiently high transverse temperatures the space-charge potential can be ignored compared with the focusing potential and we have $\rho(r)=\rho_0\exp[-U_b(r)/T_\perp]$ or

$$\rho(\mathbf{r})=\frac{eZ\exp(-r^2/2a_\perp^2)}{2\pi a_\perp^2}\delta(z) , \quad \text{(A7)}$$

where $a_\perp=[T_\perp/(m\omega_b^2)]^{1/2}$ determines the effective amplitude of transversal oscillations.

The potential of interaction of two "charged disks" (as proposed to explain the observations of the experiment of Dementev *et al.* [1]) can be evaluated by using the Fourier transform technique: Performing integration we can express the effective potential of interaction in terms of the error function [26]

$$U(z)=(eZ)^2\int_0^{\infty}\exp(-k_\perp^2a_\perp^2-|zk_\perp|)dk_\perp$$
$$=\frac{(eZ)^2\sqrt{\pi}}{2a_\perp}\exp\left[\frac{z^2}{4a_\perp^2}\right]\mathrm{erfc}\left[\frac{z}{2a_\perp}\right] . \quad \text{(A8)}$$

At $z\sim a_\perp$ this potential is much smaller than the Coulomb potential (see Fig. 3). At large distance the potential (A8) is rather Coulomb-like and in calculating the phonon frequency we must take into account the screening factor (A5). It provides for the phonon-dispersion relation

$$\omega^2(q)=\frac{2(eZ)^2}{md^3}\int_0^{\infty}dw\,w^2\exp[-w^2(a_\perp/d)^2]\left[\frac{1}{\exp(d/D+w)-1}-\frac{e^{d/D+w}\cos(qd)-1}{e^{2(d/D+w)}-2e^{d/D+w}\cos(qd)+1}\right] . \quad \text{(A9)}$$

We can use this formula for the numerical calculation of $\omega(q)$ for all q and parameters of the problem d, $a_\perp$, and D in Fig. 4.

Expanding (A9) in a power series on q and taking into account that $d/D \ll 1$ (for typical storage ring $d\sim 10^{-3}$–10^{-2} cm and $D\sim 10$ cm) we obtain at small q the soundlike dispersion relation but with

$$c_s^2=\frac{2(eZ)^2}{md}\ln(D/a_\perp) . \quad \text{(A10)}$$

*Permanent address: L. D. Landau Institute for Theoretical Physics, 117334 Moscow, Russia.

[1] E. N. Dementev, N. S. Dikanskii, A. S. Medvedko, V. V. Parkhomchuk, and D. V. Pestrikov, Zh. Tekh. Fiz. **50**, 1717 (1980) [Sov. Phys. Tech. Phys. **25**, 1001 (1980)].
[2] E. Jaeschke *et al.*, Part. Accel. **32**, 97 (1990).
[3] B. Franzke, in *Proceedings of the Particle Acceleration Conference, San Francisco, 1991* (IEEE, New York, 1991), p. 2880.
[4] S. Schröder *et al.*, Phys. Rev. Lett. **64**, 2901 (1990).
[5] I. Waki, S. Kassner, G. Birkl, and H. Walther, Phys. Rev. Lett. **68**, 2007 (1992).
[6] R. W. Hasse, Phys. Rev. A **45**, 5189 (1992).
[7] S. R. Goldman and I. Hofmann, IEEE Trans. Plasma Sci. **18**, 789 (1990).
[8] J. P. Schiffer and P. Kienle, Z. Phys. A **321**, 181 (1985).
[9] A. Rahman and J. P. Schiffer, Phys. Rev. Lett. **57**, 1133 (1986).
[10] I. Hofmann and J. Struckmeier, in *Proceedings of the Workshop on Crystalline Ion Beams, Wertheim, 1988,* edited by R. W. Hasse, I. Hofmann and D. Liesen (GSI, Darmstadt, 1989), p. 140.
[11] R. W. Hasse and J. P. Schiffer, in *Proceedings of the Workshop on Crystalline Ion Beams, Wertheim, 1988,* edited by R. W. Hasse, I. Hofmann, and D. Liesen (GSI, Darmstadt, 1989), p. 33.
[12] V. V. Parkhomchuk and D. V. Pestrikov, Zh. Tekh. Fiz. **50**, 1411 (1980) [Sov. Phys. Tech. Phys. **25**, 818 (1980)].
[13] Swapan Chattopadhyay (unpublished).
[14] D. Habs *et al.*, Nucl. Instrum. Methods B **43**, 390 (1989).
[15] S. Cocher and I. Hofmann, Part. Accel. **34**, 189 (1990).
[16] A. A. Maradudin, E. W. Montroll, G. H. Weiss, and I. P. Ipatova, *Theory of Lattice Dynamics in the Harmonic Approximation,* 2nd ed. (Academic, New York, 1971).
[17] R. Pynn, in *Methods of Computational Physics,* edited by A. Alder, S. Fernbach, and M. Rotenberg (Academic,

New York, 1976), Vol. 15, p. 41.
[18] S. A. Brasovskiĭ and I. E. Dzyaloshinskiĭ, Zh. Eksp. Teor. Fiz. **71**, 2338 (1976) [Sov. Phys. JETP **44**, 1233 (1976)].
[19] G. Radons, J. Keller, and T. Geisel, Z. Phys. B **50**, 289 (1983).
[20] S. Ichimaru, Rev. Mod. Phys. **54**, 1017 (1982).
[21] W. Slattery, G. Doolen, and H. DeWitt, Phys. Rev. A **21**, 2087 (1980).
[22] L. D. Landau and E. M. Lifschitz, *Course of Theoretical Physics,* 3rd ed. Statistical Physics Vol. 5 (Pergamon, Oxford, 1980), Part 1.
[23] F. Lindemann, Phys. Z. **11**, 609 (1910).
[24] J. A. Reissland, *The Physics of Phonons* (Wiley, London, 1973).
[25] I. S. Gradshteyn and I. M. Ryzhik, *Table of Integrals, Series, and Products* (Academic, New York, 1980).
[26] *Handbook of Mathematical Functions,* edited by M. Abramowitz and I. A. Stegun, Natl. Bur. Stand. Appl. Math. Ser. No. 55 (U.S. GPO, Washington, D.C., 1972).
[27] A. Piwinski, Stanford Linear Accelerator Center Report No. CONF740522 (1974) (unpublished).
[28] N. S. Gillis, N. R. Werthamer, and T. R. Koehler, Phys. Rev. **165**, 951 (1968).